Time-domain CMOS temperature sensors with temperature-to-digital converter

Sang Hyung Kim, Hyeon Deok Jeon, Chul Kyu Park, and Joong Ho Choi[a]
Department of Electrical and Computer Engineering, University of Seoul
E-mail: jchoi@uos.ac.kr

Abstract **- In this paper, two types of CMOS temperature sensors using temperature-to-digital converter (TDC) are proposed. The proposed circuits are suitable for low-power, small- area hardware because it is a temperature sensor made only of general MOS transistors. It is also simple to implement calibration scheme in order to obtain desired accuracy. One temperature sensor is a temperature sensor using ring oscillator with the supply voltage variation compensation scheme and the other utilizes relaxation oscillator. Each circuit was fabricated with Samsung 65nm 1P4M CMOS technology and operates over the temperature range from -40°C to 120°C. The chip area of the temperature sensor using ring oscillator and relaxation oscillator is 0.056mm^2 and 0.047mm^2, respectively.**

Keywords **—CMOS temperature sensors, Temperature-to-digital converter (TDC), Relaxation oscillator, Ring oscillator**

I. INTRODUCTION

System implementation of IoT, big data, and wearable devices, which should be one of the most important fields in IT industry these days, should be based on miniaturization, performance and portability of hardware. For all of these technologies, the role of SoC (System-on-Chip) in achieving high-density and high-efficiency energy management in the physical layer should be essential. One of the problems that has arisen with advances in modern sub-micron CMOS process is thermal issues. Continuously increasing power density has resulted in heat problems together with power consumption problems [1].

Among various solutions relieving for the thermal problem, the most efficient is to start monitoring temperature resulting from high power density environment. The generated temperature should be in a digital format and can be converted to a performance variable in order to be controlled to ensure maximum performance and efficiency with respect to voltage and process variations.

In this scheme, temperature sensor that is the core block of Hardware Performance Monitor (HPM) is designed only with the conventional MOS transistors. Various MOSFET temperature sensors have been designed to improve the resolution of temperature measurement without using bipolar junction transistors of which characteristics are difficult to be figured.

In this paper, design of two temperature sensor using basic ring oscillator and relaxation oscillator is proposed. The temperature sensor using the ring oscillator is suggested to maintain performance of the temperature sensor by including a technique for compensation of the error caused by the change of V_{DD}. In the temperature sensor using the relaxation oscillator, PTAT current and REF current are generated using MOSFETs operating in the sub-threshold region.

II. EXPERIMENTS

A. The temperature sensor using ring oscillator

In a ring oscillator consisting of N inverter stages, pulse width of the generated output and propagation delay of each inverter are (1) and (2), respectively [2,3]. The mobility of a MOSFET is inversely proportional and the V_{TH} is proportional to temperature respectively. Considering that V_{TH} is negligible compared to V_{DD}, the propagation delay in (2) is inversely proportional to mobility. Therefore, the propagation delay of CMOS inverter can be assumed to be linearly proportional to the temperature at some level and used for temperature sensors. [4]

$$Pulse\ \ Width = N \cdot 2t_p \quad (1)$$

$$\tau_p = \frac{2C_L V_{th}}{\mu C_{ox}\frac{W}{L}(V_{DD}-V_{th})^2} + \frac{C_L}{\mu C_{ox}\frac{W}{L}(V_{DD}-V_{th})} ln\left(\frac{1.5V_{DD}-2V_{th}}{0.5V_{DD}}\right) \quad (2)$$

Very large number of inverters are required in order to obtain a desired resolution with respect to operating temperature range, and this results in a problem that current consumption and chip area are greatly increased. To solve this problem, the desired operation range can be obtained using a frequency divider consisting of a D-flip flop. The divided pulse width of the ring oscillator can be converted to a digital value by starting the digital counter at the rising edge of the output pulse and loading the output counter value into the output register at the falling edge of the pulse.

As shown in (2), timing information and corresponding

a. Corresponding author; jchoi@uos.ac.kr

Manuscript Received Nov. 28, 2017, Revised Dec. 12, 2017, Accepted Dec.27, 2017

temperature measurement severely depend upon the value of power supply V_{DD}. In this paper, a reference voltage generator is proposed that can be independent upon V_{DD} and used for V_{DD} monitoring. Figure 1 shows the circuit schematic for obtaining a reference voltage independent of V_{DD} variation. V_{DD} voltage is scaled down through R_1 and R_2 and applied to the gate of the MOSFET to convert the voltage into current value. The output reference voltage is obtained in (3) and it can be independent of V_{DD} as shown in (4) when the condition in (5) can be satisfied.

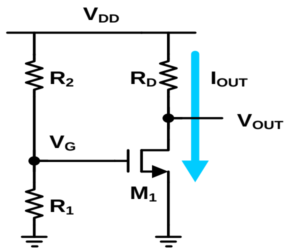

Fig. 1. Reference voltage circuit that is independent of V_{DD}.

$$V_{OUT} = V_{DD} - R_D I_{OUT} \tag{3}$$

$$\frac{\partial V_{OUT}}{\partial V_{DD}} = 1 - R_D \frac{\partial I_{OUT}}{\partial V_{DD}} = 1 - R_D \frac{\partial}{\partial V_{DD}}\left[\frac{\beta}{2}\left(\frac{R_1}{R_1+R_2}V_{DD} - V_{th}\right)^2\right] = 0 \tag{4}$$

$$\frac{R_2}{R_1} + 1 = \frac{2}{\frac{V_{th}}{V_{DD}} + \sqrt{\left(\frac{V_{th}}{V_{DD}}\right)^2 + \frac{4}{\beta R_D V_{DD}}}} \tag{5}$$

As can be seen in (5), the condition for obtaining a desired reference voltage might be varied as V_{DD} changes, and it cannot be easily realized. This is due to the non-linear voltage –current characteristic of transistor M_1 operating in the saturation region. Series feedback can be included in order to have a linear voltage-current relationship of MOSFET in the saturation region, which can be implemented by adding a degenerate resistor R_S to the source terminal of transistor M_1 as shown in Fig. 2.

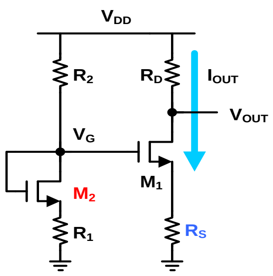

Fig. 2. Improved reference voltage circuit that is independent of V_{DD}.

This added resistor not only enhances voltage-current linearity of M_1, but also lowers trans-conductance value, allowing it to maintain this linear characteristic over a wide operating range. In addition, M_2 is used with resistors R_1 and R_2 to provide the voltage V_G to the gate terminal. This helps to maintain identical V_{GS} voltage tendency between two transistors M_1 and M_2. Figure 3 shows the simulation results of the circuit in Fig. 2. In the temperature range of -40 °C to + 120 °C, reference voltage varies larger than 200mV in absence of the M_2, but its variation can be reduced to about 6mV by adding compensation transistor M_2.

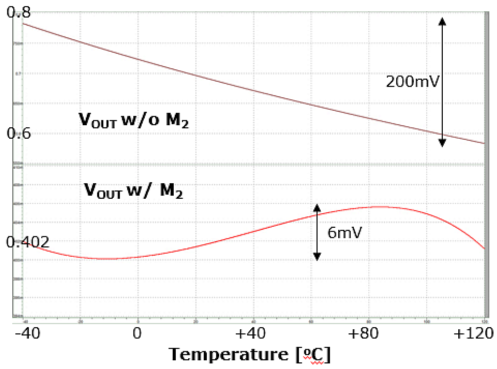

Fig. 3. Simulation results of reference voltage circuits in Fig. 1 and 2.

A block diagram of the proposed temperature sensor using ring oscillator is shown in Fig. 4, which includes a technique to compensate for error in propagation delay with V_{DD} variation. In order to compensate the propagation delay error according to V_{DD}, load capacitors controlled by a switch are added to the output of each CMOS inverter stage. As shown in Fig. 4, the controller drives the switches for load capacitance control. The controller operates for half period of the output pulse when temperature sensing does not operate. Based upon these data, the temperature sensor monitors the operating temperature during the other half period. In the proposed temperature sensing scheme, V_{DD} monitoring circuit is implemented with a reference voltage circuit that is shown in Fig. 2.

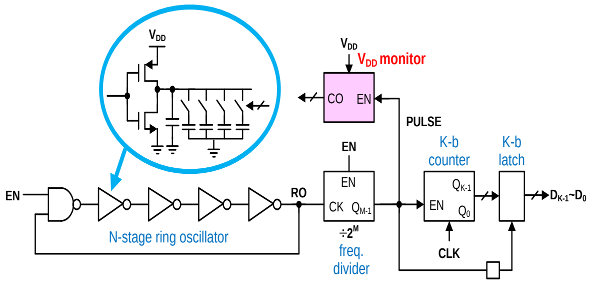

Fig. 4. Block diagram of Temperature Sensor using Ring Oscillator to correct VDD Variation.

Figure 5 shows the circuit schematic of V_{DD} monitor. In this circuit, a VDD-independent reference voltage is compared with VDD variation that is implemented with resistor ladder circuit. A digital output can be obtained by generating an output reference voltage independent of V_{DD} and comparing it with varying V_{DD} value. Similar to operations of typical Flash ADC, the thermometer code is generated by comparing several scaled V_{DD} values with reference value. A decode logic is used to control the switch needed for each stage of the ring oscillator. In our design, only four levels of load capacitor control are included, which can cover variation range of +/- 10%. In order to improve the accuracy of V_{DD}-variation compensation, more comparators can be used to generate more control bits.

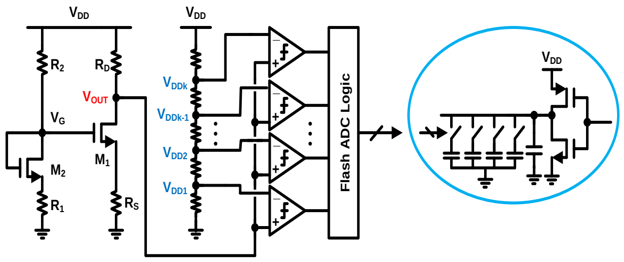

Fig. 5. Circuit schematic of V_{DD} monitor.

Simulation results of the temperature sensor in Fig. 4 are shown in Fig. 6. The simulation results were obtained by varying V_{DD} voltage from 1.0V to 1.4V. With the calibration data at 20 °C of compensation scheme in Fig. 5, pulse width variation is significantly reduced from 11 μsec (42.3%) to 2 μsec (7.7%).

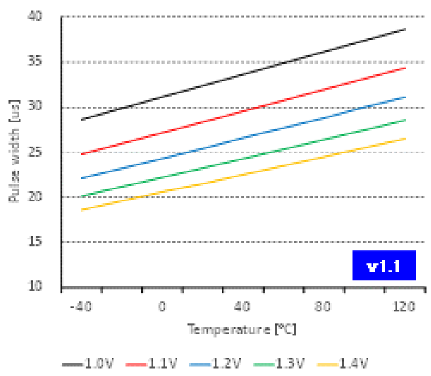

(a)

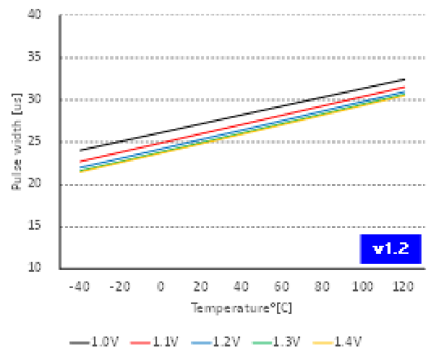

(b)

Fig. 6. Simulation results of temperature sensor using ring oscillator (a) Output pulse width change simulation of a circuit that does not use the supply voltage compensation technique, (b) Output pulse width change simulation with compensation technique.

B. The temperature sensor using relaxation oscillator

The output of the pulse generated by the relaxation oscillator can be generally obtained by

$$T_{OUT} = \frac{C \cdot V}{I} \tag{6}$$

where V and I are capacitance voltage and charging current, respectively.

In a conventional temperature sensor using a relaxation oscillator, the current I has a PTAT (proportional-to-absolute-temperature) characteristic and V should have a temperature-independent characteristic. Therefore, there might be a problem that the digital output value is inversely proportional to the temperature or frequency should be monitored instead of time information. In addition, the reference voltage V is very difficult to internally obtain without bipolar junction transistors or external voltage source [5]. In this paper, the output pulse characteristic of (6) is designed to be proportional to the temperature by making the charging current be independent of the temperature and having the reference voltage V with the PTAT characteristic. Thus, by changing (6), the output linearly proportional to the temperature can be obtained as follows.

$$T_{OUT} = \frac{C \cdot R \cdot I_{PTAT}}{\alpha I_{PTAT} + \beta I_{CTAT}} \tag{7}$$

Here, R is a device that converts the PTAT current to the PTAT voltage, and the values of α and β are parameter values that can produce a temperature-independent current through a combination of PTAT current and CTAT current. The oscillator can be operated in the current domain to obtain the characteristics independent of the V_{DD}, and the nonlinearity of the PTAT current.

A block diagram of the proposed temperature sensor using a relaxation oscillator is shown in Fig. 7. The current generated in the I_{PTAT} block is coupled to the R_{PTAT} through the current mirror to form V_{PTAT}. The current generated in the I_{CTAT} block can be combined with the I_{PTAT} current in C_{RAMP} to obtain temperature-independent integration characteristics. This temperature sensor operates asynchronously to the SEN signal, which is an external control signal, so that current consumption can be greatly reduced. That is, if SEN signal is generated as a pulse, one temperature sensing operation is performed, and after the digital value is loaded in the output register, all the blocks become idle and no current consumption occurs.

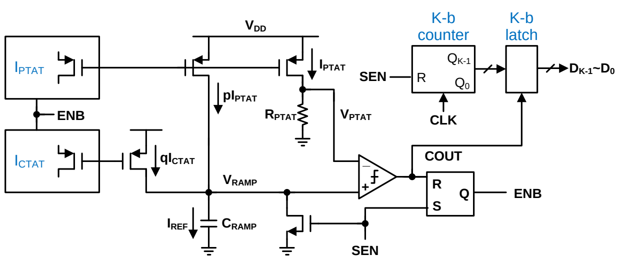

Fig. 7. Block diagram of the proposed temperature sensor using relaxation oscillator.

The timing diagram of this temperature sensor is shown in Fig. 8. When the external SEN signal (temperature sensing start signal) is applied, the status of RS latch is set, which is used as the enable signal of the whole block. When SEN signal falls to 0, the reset switch of the C_{RAMP} is opened and the integrating operation begins. When the integral value of this capacitor is equal to V_{PTAT}, the state of the comparator is changed. The output of this comparator controls the operation of the output counter to measure the pulse width from the falling edge of the SEN signal to the moment when the output of the comparator changes. After that, the state of RS latch becomes reset state and all blocks are disabled.

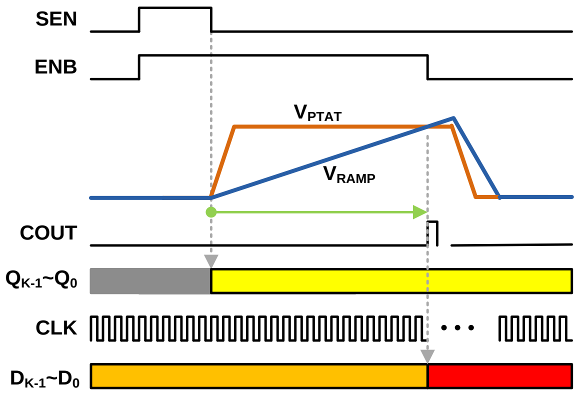

Fig. 8. Timing diagram of the proposed temperature sensor using relaxation oscillator.

The circuit schematic for obtaining the CTAT current of Fig. 7 is shown in Fig. 9. When a transistor M_1 is used in the weak-inversion region, the current equation is as follows.

$$I_{DS} = I_{DSO} \cdot e^{\frac{V_{GS}}{nV_T}} \cdot \left(1 - e^{-\frac{V_{DS}}{V_T}}\right) \tag{8}$$

In general, since $V_{DS} >> V_T$, the relationship between V_{GS} and current has an exponential characteristic similar to that of BJT [6-7]. At this time, the output current I_{CTAT} is

$$I_{CTAT} = \frac{V_{GS1}}{R_{B2}} \tag{9}$$

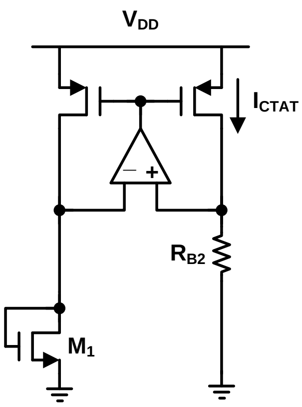

Fig. 9. Current generating circuit with CTAT characteristics.

The circuit that generates the current with the PTAT characteristic is shown in Fig. 10. Using the two transistors M_1 and M_2 operating in the weak-inversion region, (the multiple ratio of the transistor = 1: N), a thermal voltage is generated, which can be obtained through the resistor R_{B1} as follows,

$$I_{PTAT} = \frac{V_{GS1} - V_{GS2}}{R_{B1}} = \frac{k \cdot nV_T}{R_{B1}} \tag{10}$$

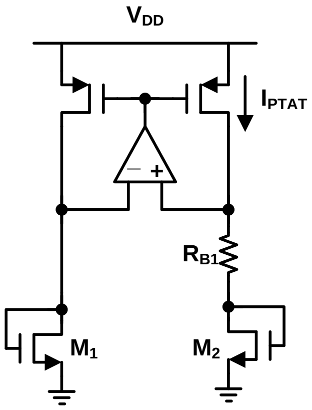

Fig. 10. Current generating circuit with PTAT characteristics.

Under the normal condition (V_{DD} = 1.2V, TT process), simulation results for the temperature sensor is shown in Fig. 11. As the temperature rises, leakage currents generated in many transistors (in particular, a C_{RAMP} reset switch) might degrade performance of the sensor, a method of compensating the leakage current of each block is required. At -40 °C, the pulse width is 28.1 us, and at 120 °C, it is 41.5 us. Therefore, the pulse width in the operating range is 13.4 us. When the external clock used for the output counter is 57 MHz, the number of outputs that can be counted within the operating range is 766. The resulting resolution is 0.21 °C and the total number of digital output bits, including an offset of -40 °C, is 12 bits.

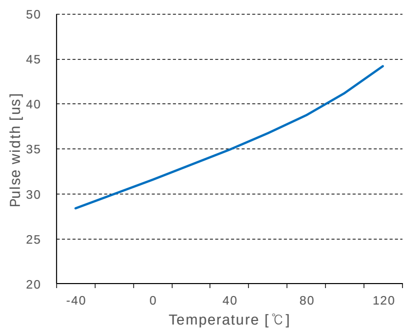

Fig. 11. Simulation results of temperature sensor using relaxation oscillator.

III. RESULTS AND DISCUSSION

Figure 12 shows the output frequency measurement waveform of a ring oscillator with the supply voltage variation compensation technique. Figure 12(a), (b) and (c) present frequency waveforms when the supply voltages are 1.1 V, 1.2 V and 1.3 V, respectively. The output frequency is approximately 17.91 kHz at a supply voltage 1.2V. With compensation method of the proposed V_{DD} monitoring circuit, the output frequencies are 17.34 kHz or 18.34 kHz, respectively, with an error of about 3% or less.

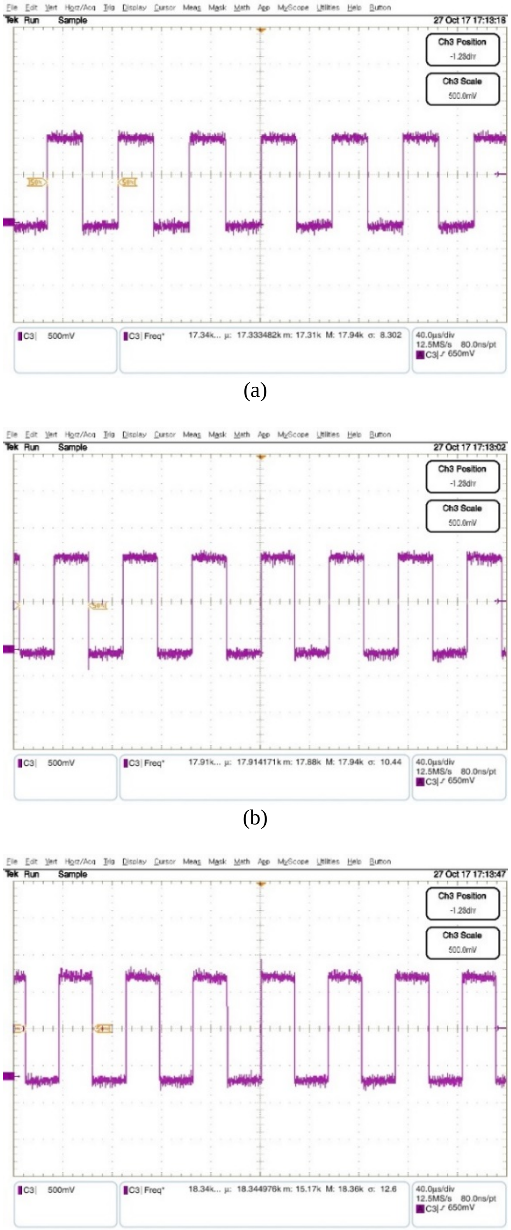

(a) (b) (c)

Fig. 12. Measurement results of ring oscillator output (a) at supply voltage of 1.1V, (b) at 1.2V and (c) at 1.3V.

The proposed CMOS temperature sensor is measured at room temperature, 27° C. The measurement environment consists of a supply voltage of 1.2 V and external reference frequency of 57 MHz. Figure 13(a) presents the output code of the proposed temperature sensor through a logic analyzer. The output code value is 1589, which shows an error of less than 10% when compared with the simulation result value of 1478.

At room temperature, the measurement of the temperature sensor using the relaxation oscillator is shown in Fig. 13(b). The digital code measured by the logic analyzer is 2040, with an error of 5.9% compared to the simulation result.

The temperature sensor is designed using a 65nm CMOS process, and the layout of each IP is shown in Fig. 14. The performances of temperature sensors are summarized in Table II.

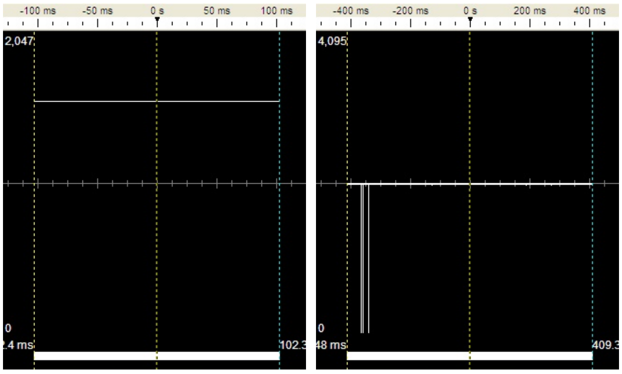

(a) (b)

Fig. 13. digital output measurement result of the temperature sensor at 27° C. (a) Using ring oscillator (b) Using relaxation oscillator

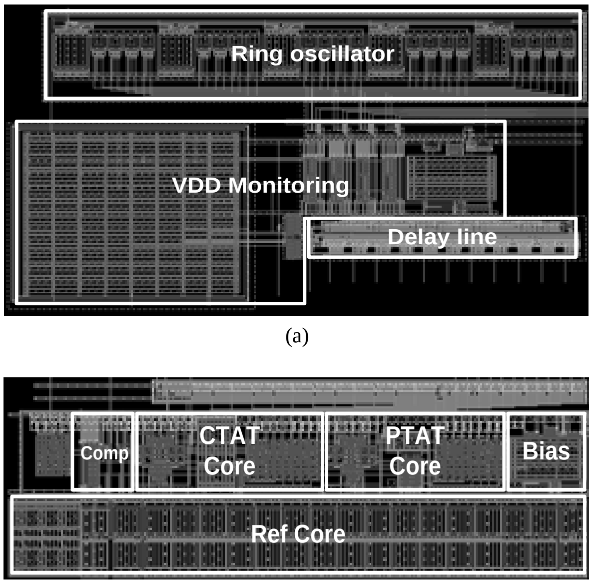

(a) (b)

Fig. 14. Layout of the proposed temperature sensor. (a) Temperature sensor using ring oscillator (b) Temperature sensor using relaxation oscillator

TABLE II
Performance comparison among temperature sensors

Specification	This work A	This work B	[2]	[4]	[5]
Technology (nm)	65	65	350	65	180
Temperature range (°C)	-40-120	-40-120	0-100	0-60	-10-30
Resolution (°C)	0.31	0.21	0.16	0.139	0.2
Conversion rate (SPS)	27.8k	20k	10k	10k	333
Power consumption (uW)	144	86	10	150	0.119
Area (mm^2)	0.056	0.047	0.175	0.01	0.0416

IV. CONCLUSION

In this paper, two temperature sensors using ring oscillator and relaxation oscillator are presented. In the case of a temperature sensor using a ring oscillator, a V_{DD} monitoring circuit capable of compensating variation of V_{DD} power supply has been implemented to improve accuracy performance. The temperature sensor using the relaxation oscillator utilize the characteristics that behave like a BJT with MOSFETs operating in the sub-threshold region. Since the leakage current increases as the temperature increases, a method for compensating this leakage current is needed.

ACKNOWLEDGMENT

This work was supported by the IDEC (IC Design Education Center). This work was also supported by the R&D program of MOTIE/KEIT. [10080364, Development of a High Efficient Energy Hub System for IoT Devices]

REFERENCES

[1] R. Ronen, A. Mendelson, K. Lai, Shih-Lien Lu, F. Pollack, and J. P. Shen, "Coming Challenges in Microarchitecture and Architecture," Proceedings of the IEEE, vol.89, issue 3, pp.325-340, Mar. 2001.
[2] Chen, Poki, et al. "A time-to-digital-converter-based CMOS smart temperature sensor." IEEE Journal of Solid-State Circuits 40.8 (2005): 1642-1648.
[3] T. A. Demassa and Z. Ciccone, Digital Integrated Circuits. New York: Wiley, 1996.
[4] SHIM, Daeyong, et al. A process-variation-tolerant on-chip CMOS thermometer for auto temperature compensated self-refresh of low-power mobile DRAM. IEEE Journal of Solid-State Circuits, 2013, 48.10: 2550-2557.
[5] Law, Man Kay, Amine Bermak, and Howard Cam Luong. "A sub-μW embedded CMOS temperature sensor for RFID food monitoring application." IEEE Journal of Solid-State Circuits 45.6 (2010): 1246-1255.
[6] M. S. Floyd et al., "System power management support in the IBM POWER6 microprocessor," IBM J. Res. Develop., pp.733–746, Nov. 2007.
[7] Lin, Yu-Shiang, Dennis Sylvester, and David Blaauw. "An ultra-low power 1V, 220nW temperature sensor for passive wireless applications." 2008 IEEE Custom Integrated Circuits Conference. IEEE, 2008.

Sanghyung Kim was born in Seoul, Korea, in 1991. He received the B.S. degree in electrical engineering from University of Seoul, Seoul, Korea, in 2016. He is currently working toward the M. S. degree at the same university.

His research interest include design of high performance analog integrated circuits.

Hyeondeok Jeon was born in Gwangyang, Korea, in 1989. He received the B.S. degree in electrical engineering from University of Seoul, Seoul, Korea, in 2016. He is currently working toward the M. S. degree at the same university.

His research interest include design of high performance analog integrated circuits.

Chulkyu Park was born in Daejeon, Korea, in 1984. He received the B.S. and the M.S. degrees in electrical engineering from University of Seoul, Seoul, Korea, in 2010, 2012, respectively. He is currently working toward the Ph. D. degree at the same university.

His research interest include design of high performance analog integrated circuits.

Joongho Choi was born in Korea, in 1964. He received the B. S. and the M. S. degrees in electronics engineering from Seoul

National University, Seoul, Korea, in 1987, 1989, respectively. He received the Ph.D. degree in electrical engineering from University of Southern California, California, in 1993. From 1994 to 1996, he worked at IBM T. J. Watson Research Center in Yorktown Heights, NY, where his research was to implement the parallel optical interconnection system. He joined University of Seoul, Seoul, Korea in 1996, where he is currently an Associate Professor. He has published more than 45 papers in international journal and conference proceedings.

His main research areas include mixed-signal VLSI designs for signal processing and high-speed data transmission.